

# The shock layer thickness, a new approach to the study of column performance in non-linear chromatography

## I. Optimum linear velocity in frontal analysis

Jie Zhu and Georges Guiochon\*

Department of Chemistry, University of Tennessee, Knoxville, TN 37996-1600 (USA) and Division of Analytical Chemistry, Oak Ridge National Laboratory, Oak Ridge, TN 37831-6120 (USA)

(First received July 22nd, 1992; revised manuscript received December 16th, 1992)

---

### ABSTRACT

In non-linear chromatography, it is common to observe very steep profiles. This happens for overloaded elution bands, for frontal analysis breakthrough curves and for the band profiles of the isotachic train in displacement chromatography. These regions where the concentration vary very rapidly are called shock layers. The relationship between the thickness of the shock layer in frontal analysis and the coefficients of the conventional terms of the plate height equation were studied experimentally. The shock layer theory of Rhee and co-workers permits the simple determination of the optimum linear velocity for minimum shock layer thickness in the case when the adsorption behavior of the feed components is described by the Langmuir model. The optimum linear velocity in frontal analysis is not only a function of the coefficients of the axial dispersion and the mass transfer resistance terms, and the retention factor ( $k'_0$ ), as in linear chromatography, but also a function of the plateau concentrations and the second Langmuir parameter of the isotherm,  $b$ . Depending on the retention factor, the optimum velocity in frontal analysis may be larger, but is most often much smaller than in linear chromatography. Experimental results are in excellent agreement with the prediction of the theory. If they could be extended to displacement chromatography, these findings would explain some apparent contradictions found in the literature regarding the influence of the mobile phase flow velocity on the degree of separation between bands achieved in displacement chromatography, and clarify certain controversies.

---

### INTRODUCTION

In spite of a number of investigations [1–12], there is still a profound misunderstanding of the exact influence of the column efficiency on the band profiles in non-linear chromatography. Some workers are still mistaking the effects of thermodynamics caused by the non-linear behavior of the isotherm for a source of band broadening similar to axial dispersion [1,2].

Others have attempted to contrive empirical approaches which lack a fundamental background and have failed [2–4]. Knox and Pyper [5] suggested calculating the band width in non-linear chromatography by using the rule of variance additivity and applying it to two independent contributions, of kinetic and thermodynamic origin, respectively. The former contribution is derived from the column efficiency, the latter from an approximate solution of the ideal model [5]. This procedure gives a reasonable estimate of the band width [6–8] and a very good approximation of the profile of the dispersive boundary of the profile. However, it is not correct because the convolution of the thermo-

---

\* Corresponding author. Address for correspondence: Department of Chemistry, University of Tennessee, Knoxville, TN 37996-1600, USA.

dynamic band profile by an axial dispersion is a shift-variant convolution [9], and the rule of variance additivity does not apply. It would fail entirely if it were used to predict the steep parts of band profiles.

We know that when the adsorption isotherm is convex upwards the band profile has a steep front and a rear diffuse boundary. (The converse is true for a convex downwards isotherm; we shall not discuss here this infrequent case.) The mechanism of the formation of such a profile was elucidated long ago [13,14], and the work done in this area was reviewed recently [10,11]. The formation of a shock in the case of an infinitely efficient column is easily explained [10–14]. When the column has a finite efficiency, the concentration discontinuity is relaxed and replaced by a steep front which is also a constant pattern, *i.e.*, propagates at the same velocity as the shock, without changing shape, and most notably without broadening [15,16]. Similarly, in frontal analysis the breakthrough curve has a very steep front, and in displacement chromatography the boundary between two successive zones is very steep. These steep boundaries are called shock layers. The theory of shock layers has been reviewed by Vermeulen *et al.* [16], who pioneered its development [17]. The simplest and most useful model has been derived and studied by Rhee and co-workers [18–21]. This theory results in a simple expression for the shock layer thickness (SLT) in the case of Langmuir adsorption behavior [18,22,23].

We present here the results of a theoretical and experimental investigation of the dependence of the SLT in frontal analysis on the two main parameters which control it, the mobile phase velocity and the height of the concentration step injected into the column. At this stage, the shock layer theory applies only in cases where a constant state, *i.e.*, a constant concentration, is achieved behind the shock layer, and thus the ideal shock would move at a constant velocity. This is the case in frontal analysis, after the time needed for the constant state to be established [22]. This is also the case in displacement chromatography, when the isotachic train is formed, but the theory of shock layer in two-component cases is more complex

[21], and this topic will be discussed in a future paper [24]. However, our present results and conclusions cannot be extended directly to the study of band profiles in overloaded elution.

The determination of SLT is a new approach to the study of column performance in non-linear chromatography, which is valid when the adsorption behavior of the components considered is closely enough approximated by the Langmuir model. There is in this instance a simple relationship between the SLT and the column height equivalent to a theoretical plate (HETP). Thus, we can derive simply the optimum linear velocity for minimum SLT,  $u_{\text{opt}}^{\text{S}}$ , which is related to the optimum velocity for minimum HETP,  $u_{\text{opt}}^{\text{L}}$ . The SLT,  $\text{SLT}_{\text{min}}$  and  $u_{\text{opt}}^{\text{S}}$  will play in frontal analysis (and probably also in displacement chromatography [24]) a role similar to that of  $H$ ,  $H_{\text{min}}$ , and  $u_{\text{opt}}^{\text{L}}$  in elution chromatography.

Although constant pattern behavior, the characteristics of the breakthrough curves and the thickness of shock layers have been actively studied in chemical engineering [13–21], there has been little application of the shock layer theory so far in chromatography regarding the optimization of the experimental conditions in order to improve the steepness of the breakthrough curves in single-component frontal analysis. This is not surprising, as these fronts are already very steep anyway; the only practical use of frontal analysis is in the determination of the retention time of the inflection point of the breakthrough curve, to calculate the integral mass balance of adsorption in the column; in practice, the accuracy of this determination does not depend much on the front steepness. As shown previously, this is not entirely true in two-component frontal analysis [22].

It is more surprising that there has been a little investigation regarding the optimization of the experimental conditions to minimize the SLT in displacement chromatography and to improve zone separation in the isotachic trains. We know that the side profiles of these zones cannot be vertical, as predicted by the ideal model. Because of the axial dispersion and the finite rate of mass transfer, mixed regions appear between successive bands of pure components. These regions are shock layers. Obviously, the smaller

the shock layer thickness, the less is the degree of overlap between the bands of the isotachic train and hence the better is the separation. Actually, there are contradictory reports regarding the influence of the linear velocity on the quality of the separations achieved in displacement chromatography [25–31]. Although this paper does not address this important problem, it is the first and necessary step in this direction. The solution of single-component problems is simpler and easier to study than that of multi-component problems.

## THEORY

This work is based on the shock layer theory of Rhee and co-workers [18–21]. The model they used considers the constant pattern behavior [15–21], which is an asymptotic solution, *i.e.*, is achieved only after an infinitely long migration along the column. One of the problems encountered in the application of this theory will be to determine whether a constant pattern is achieved at elution. The basic assumptions of the model are (i) the additivity of the dispersive contributions from finite mass transfer rates and from axial dispersion (axial and eddy diffusions); and (ii) the approximation of the mass transfer kinetics by the solid film linear driving force model. Because of the high column efficiency, *i.e.*, of the fast rate of the mass transfer kinetics, the error introduced by the first assumption is certainly small. It seems that the second assumption is also valid in most cases of importance in chromatography [32].

We have recently shown how this theory can be applied to the study of the very steep fronts observed in high-concentration chromatography [22,23]. We first recall the definition of the SLT, then summarize the previous results and finally derive the relationships between the SLT, the mobile phase flow velocity and the displacer concentration in the case of Langmuir isotherm behavior.

### Definition of shock layer thickness

In frontal analysis, a concentration step of constant height propagates along the column. The concentration profile at the column exit, or

breakthrough curve, is the column response to a step input. It becomes ideally flat only at infinite distances from the center of the shock layer while we are interested in the part of the profile within a finite region. Thus, it is useful to define two concentrations bounds  $C_r^*$  and  $C_l^*$ , and an auxiliary variable  $\theta$ , as:

$$\theta = \frac{C^l - C_l^*}{C^l - C^r} = \frac{C_r^* - C^r}{C^l - C^r} \quad (1)$$

where  $C^l$  and  $C^r$  are the concentrations in the column at  $x = -\infty$  and  $x = +\infty$ , respectively. The definition of  $\theta$  is illustrated in Fig. 1. The thickness of the shock layer is defined as the distance between the concentration bounds  $C_r^*$  and  $C_l^*$ :

$$\Delta\eta_x = x(C_l^*) - x(C_r^*) \quad (2)$$

$\Delta\eta_x$  depends on the choice of the arbitrary number  $\theta$ , which in frontal analysis plays the same role as the relative peak height in elution. In this work we have taken  $\theta = 0.02$ . In displacement chromatography (which we shall discuss in a future paper [24]) and in many frontal analysis experiments (including all those performed in this work),  $C^r = 0$  (the column does not contain any solute before the experiment starts), and  $C^l = C_0$ . Then,  $C_r^* = \theta C_0$  and  $C_l^* = (1 - \theta)C_0$ .

Rhee and co-workers [18–20] considered reduced (*i.e.*, dimensionless) variables, including a moving coordinate,  $\xi = x - \lambda\tau$ , with  $x = z/L$ , reduced distance,  $\tau = ut/L$ , reduced time, and  $\lambda$ , reduced shock velocity  $\{\lambda = 1/[1 + F(\Delta Q/\Delta C)]\}$ . They calculated the reduced SLT,  $\Delta\xi$ , along the direction  $\xi$  of migration of the shock in the  $x,t$  plane. The SLT at the column exit ( $z = L$ ) is given by [23]:

$$\Delta\eta_x = L \Delta\xi \quad (3a)$$

where  $L$  is the column length. The SLT in time units at the column exit (elution) is given by:

$$\Delta\eta_t = \frac{L}{U_s} \cdot \Delta\xi \quad (3b)$$

where  $U_s$  is the shock velocity:

$$U_s = \frac{u}{1 + F \cdot \frac{\Delta Q}{\Delta C}} \quad (4)$$

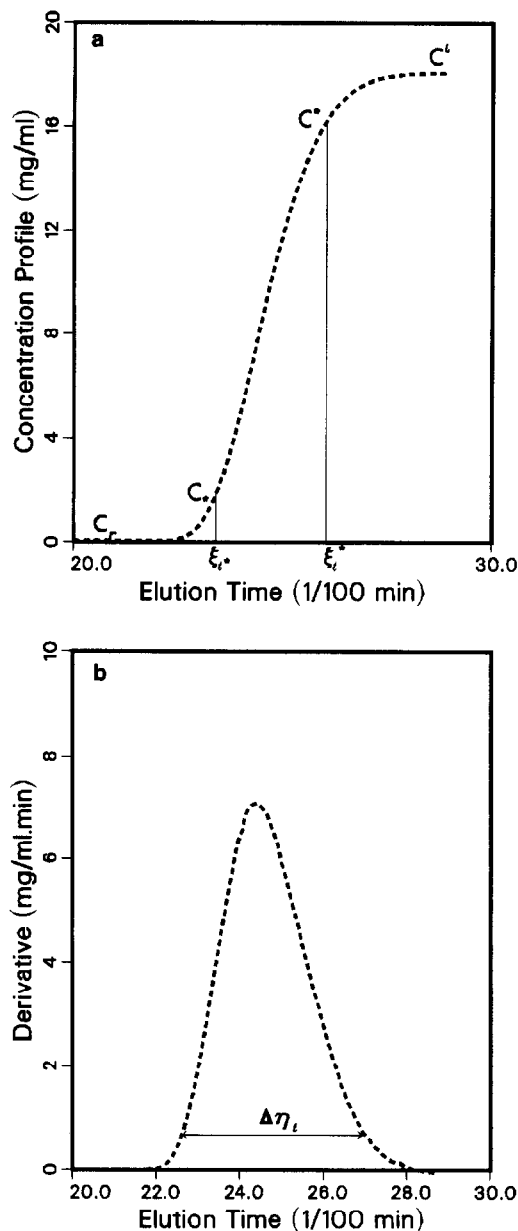


Fig. 1. Definition of  $\theta$  and other parameters used to study the shock layer. (a) Breakthrough curve corresponding to a single component step. (b) Differential of the breakthrough curve corresponding to a single-component step.

where  $u$  is the mobile phase velocity and  $\Delta Q$  and  $\Delta C$  are the amplitude of the concentration jumps in the stationary and the mobile phases, respectively.  $Q$  and  $C$  are related by the isotherm equation,  $Q = f(C)$ , so the amplitudes of the

concentration jumps are  $\Delta Q = Q_1 - Q_r = f(C_1) - f(C_r)$  and  $C_1 - C_r$ , respectively, if  $C_1$  and  $C_r$  are the mobile phase concentrations after and before the jump, respectively.

Obviously, the shock layer thickness is a function of  $\theta$ .

#### Thickness of the shock layer

Rhee and Amundson [19] assumed that the zone dispersion in the column results from two phenomena, axial dispersion due to molecular and eddy diffusion and characterized in chromatography by the first two terms of the Van Deemter [33] or the Knox [34] equations, and mass transfer resistance characterized by the third term of these equations. They showed that a constant pattern (shock layer) forms and propagates at the same velocity as the shock of the ideal model. They then derived an equation giving the profile of concentration in the shock layer of a pure component [19]. In the case of a Langmuir isotherm [18], this equation gives for the shock layer obtained when the concentration varies from 0 to  $C_0$ :

$$\Delta\xi = \left[ \frac{D_L(1+K)}{KuL} + \frac{u}{(1+K)k_fL} \right] \frac{\Gamma_0 + 2}{\Gamma_0} \cdot \ln \left| \frac{1-\theta}{\theta} \right| \quad (5a)$$

$$\Delta\eta_x = \left[ \frac{D_L(1+K)}{Ku} + \frac{u}{(1+K)k_f} \right] \frac{\Gamma_0 + 2}{\Gamma_0} \cdot \ln \left| \frac{1-\theta}{\theta} \right| \quad (5b)$$

$$\Delta\eta_t = \left[ \frac{D_L(1+K)^2}{Ku^2} + \frac{1}{k_f} \right] \frac{\Gamma_0 + 2}{\Gamma_0} \cdot \ln \left| \frac{1-\theta}{\theta} \right| \quad (5c)$$

where  $D_L$  is the axial dispersion coefficient, including the effects of molecular axial diffusion, tortuosity and eddy diffusion, and  $k_f$  is the rate constant of mass transfer (solid film driving force model [19]). Note that in the equilibrium-dispersive model, the apparent dispersion coefficient denoted  $D_a$  and used in previous papers [32] includes also the effect of mass transfer kinetics; here it does not, which is why we use a different symbol. Eqn. 5a is dimensionless and eqns. 5b

and  $c$  give the SLT in length and time units, respectively. The equation 5b is the most practical for comparison with experimental results.

In these equations, the Langmuir isotherm is written as

$$q = \frac{ac}{1 + bC} = \frac{bq_s C}{1 + bC} = \frac{q_s \Gamma}{1 + \Gamma} = q_s \Lambda \quad (6a)$$

$$\Lambda = \frac{\Gamma}{1 + \Gamma} \quad (6b)$$

where  $Q$  and  $C$  are the actual concentrations of the compound in the stationary and the mobile phases, respectively,  $q_s$  is the specific saturation capacity of the adsorbent,  $a$  and  $b$  are numerical coefficients and  $\Lambda = q/q_s$  and  $\Gamma = bc$  are dimensionless concentrations; when  $\Gamma = 1$ , the amount adsorbed at equilibrium is  $\Lambda = 0.5$ . Accordingly,  $\Gamma_0 = bC_0$ . The parameter  $K$  in the eqns. 5 is

$$K = \frac{k'_0}{1 + \Gamma_0} \quad (7)$$

where  $k'_0$  is the retention factor, proportional to the initial slope of the isotherm ( $k'_0 = Fa = Fbq_s$ ; see eqn. 6a). Finally, we note that the shock velocity in the conventional case when  $C_r = 0$  and  $C_i = C_0$  can be written as

$$U_s = \frac{u}{1 + \frac{Fbq_s}{1 + \Gamma_0}} = \frac{u}{1 + K} \quad (8)$$

As shown by Rhee and Amundson [19], and discussed recently [32], the band profiles calculated with the equilibrium–dispersive model and the solid film driving force model are the same provided that we use the following equation for the HETP:

$$H = \frac{2D_a}{u} = \frac{2D_L}{u} + 2 \cdot \frac{K}{(1 + K)^2} \cdot \frac{u}{k_f} \quad (9)$$

where  $D_a$  is the apparent dispersion coefficient [32,35] and  $K$  is given by eqn. 7. Eqn. 9 provides a relationship between the apparent dispersion coefficient and the concentration. The assumptions on which it is based have been discussed above. The study of the dependence of the shock layer thickness on the velocity,  $u$ , and the concentration,  $C_0$ , provides the only direct method of determination of  $H$ . In the case of linear

chromatography, this equation becomes a form of the classical plate height equation:

$$H = \frac{2D_L}{u} + \frac{2k'_0 u}{(1 + k'_0)^2 k_f} \quad (10)$$

Depending on the relationship between  $D_L$  and  $u$  which is used to account for eddy diffusion, we obtain the Van Deemter [33] or the Knox [34] plate height equations:

$$H = A + \frac{B}{u} + Cu \quad (11a)$$

$$H = \frac{B}{u} + Au^{1/3} + Cu \quad (11b)$$

with

$$2D_L = Au + B \quad (12a)$$

or

$$2D_L = B + Au^{4/3} \quad (12b)$$

and

$$C = \frac{2k'_0}{(1 + k'_0)^2 k_f} \quad (12c)$$

In eqns. 11 and 12,  $B$  is usually assumed to be equal to  $2\gamma D_m$  [33,34], where  $\gamma$  is the packing tortuosity and  $D_m$  the mobile phase diffusivity of the solute. We note that eqn. 12c was derived by Giddings [36] using a completely different approach.

## EXPERIMENTAL

### Equipment

The modular liquid chromatograph used for the measurements of the SLT was assembled from two Gilson (Middleton, WI, USA) Model 302 pumps, a Valco (Houston, TX, USA) tenport pneumatically actuated valve connected with a 1-ml loop and a Spectroflow 757 variable-wavelength UV detector (Kratos, Ramsey, NJ, USA). The detector output signal was connected to a DATA Master Model 621 (Gilson) for discretization of the response. This response was then acquired on a microcomputer, handled using the Gilson 715 software, and uploaded, when needed, on one of the computers of the University of Tennessee Computer Center.

### Columns and chemicals

A 5 × 0.46 cm I.D. Vydac (Separation Group, Hesperia, CA, USA) 5- $\mu$ m Protein & Peptide C<sub>18</sub> column, and two other columns, 5 × 0.21 cm I.D. and 25 × 0.21 cm I.D., laboratory packed with 10- $\mu$ m Protein & Peptide C<sub>18</sub>, were used.

2-Phenylethanol was purchased from Fluka (Buchs, Switzerland), 4-*tert.*-butylphenol from Aldrich (Milwaukee, WI, USA) and HPLC-grade water and methanol from Burdick and Jackson (Muskegon, MI, USA). All these chemicals were used as received.

### Procedures

**Chromatographic experiments.** The experiment was designed to reduce the amount of sample needed, so the injection of a wide rectangular pulse was substituted for a step injection. The columns were first equilibrated for 10 min with a mobile phase stream [methanol–water (50:50)] originating from one of the pumps. Then, the ten-port valve was actuated for the time needed to let the other pump push the sample plug contained in the 1-ml loop through the column and the pure mobile phase stream was resumed. Although the retention volume of the breakthrough curve exceeds 1 ml, a plateau at the injected concentration was always reached before the negative breakthrough curve started. The operation was repeated at different flow-rates and with the three columns.

**Measurement of column efficiency.** The efficiencies of the two 5-cm long columns were measured under linear conditions as a function of the mobile phase flow velocity. The results are reported in the Figs. 2 (Vydac column, with 2-phenylethanol) and 3 (laboratory packed column, with 4-*tert.*-butylphenol). The experimental data were fitted to the Van Deemter equation [33] (eqn. 11), which gave a smaller residual than the Knox equation [34] (eqn. 11b) in this instance. The values of the coefficients  $D_L = 0.5(A + B/u)$  and  $k'_t = 2k'_0/(1 + k'_0)^2 C$  derived from the fit, together with the retention factors,  $k'_0$ , are given in Table I.

**Measurement of adsorption isotherm.** The adsorption isotherms of 2-phenylethanol and 4-*tert.*-butylphenol on the three columns used were measured by frontal analysis, as described

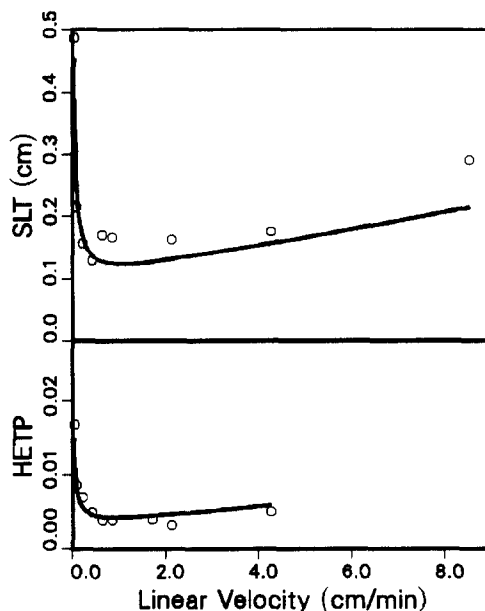


Fig. 2. Comparison between the dependences of the HETP (cm) measured under linear elution conditions and of the SLT (cm) for 2-phenylethanol on the mobile phase flow velocity. Top: plot of the SLT versus the mobile phase flow velocity. Experimental data (symbols) and prediction of eqn. 5b (solid line). Bottom: plot of the HETP versus the mobile phase velocity. Experimental data (symbols) and best fit to the Van Deemter equation (solid line). Experimental conditions (both plots): 5 cm long Vydac column; mobile phase; methanol–water (50:50), detection at 270 nm; sample, 2-phenylethanol; height of the concentration step in frontal analysis, 20 mg/ml; sample size for linear elution peaks, 40  $\mu$ g (0.2  $\mu$ l of a 20 mg/ml solution).

previously [37]. The experimental data were fitted to a Langmuir isotherm. There was excellent agreement between the experimental data and the Langmuir model in both instances. The retention factors of 2-phenylethanol and 4-*tert.*-butylphenol are 0.88 and 10.0, respectively.

**Measurement of shock layer thickness.** In principle, two procedures are available for these measurements. In the direct procedure, following the definition of the shock layer, we measure the distance between the moments when the signal reaches two selected fractions (e.g., 5 and 95%) of the baseline shift corresponding to the elution of the concentration step. Alternately, the breakthrough curves could be differentiated and their widths at a certain fractional height (e.g., half-height) taken as a measure of the

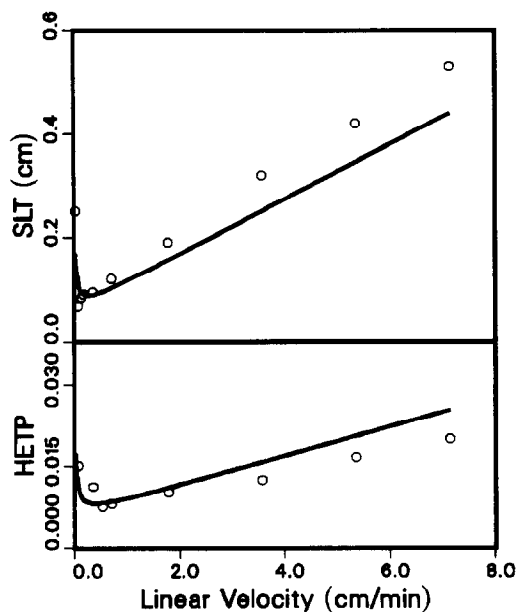


Fig. 3. Comparison between the dependences of the HETP (cm) measured under linear elution conditions, and of the SLT (cm) for 4-*tert.*-butylphenol on the mobile phase flow velocity. Plots as in Fig. 2. Experimental conditions (both plots): 5 cm long laboratory made column; mobile phase, methanol–water (50:50); detection at 276 nm; sample, 4-*tert.*-butylphenol; height of the concentration step in frontal analysis, 20 mg/ml; sample size for linear elution peaks, 0.2  $\mu$ g.

shock layer width. Both procedures require smoothing of the response signal before the measurement is carried out, in order to eliminate the signal noise.

In the first procedure, the recorded chromatogram is first smoothed using a thirteen-point floating average algorithm. Then, the times at which the filtered breakthrough curve reaches the fractions 2% and 98% of the value corre-

sponding to the plateau are determined by interpolation. These values correspond to  $\theta = 0.02$  in eqns. 5. The distance between these two times is taken as the thickness of the shock layer. This choice of  $\theta$  is arbitrary and made for the sake of convenience: any value between 0 and 0.5 would be possible. A compromise has to be found between the choices of a small value of  $\theta$ , giving a large shock layer thickness, potentially more accurate, and of a large value of  $\theta$ , corresponding to values of the detector signal which are sufficiently different from 0 and  $C_0$  and can be measured more precisely, because the slope of the signal is more important.

In the second procedure, the differential of the chromatogram is calculated by taking the difference between successive data points on the recorded chromatogram and dividing by the data acquisition period. The differential chromatogram is smoothed using a thirteen-point floating average algorithm. The points on the differential profile corresponding to the fractional heights  $\theta$  and  $1 - \theta$  on the breakthrough curve are obtained at time  $\tau_1$  and  $\tau_2$ , respectively, so that

$$\int_0^{\tau_1} y(t) dt = \theta \quad (13a)$$

$$\int_0^{\tau_2} y(t) dt = 1 - \theta \quad (13b)$$

Calibration has shown that the values of  $\tau_i$  that correspond to a given value of  $\theta$  correspond approximately to a fractional height of 10% of the derivative signal. This value changes little with the characteristics of the shock layer, *e.g.*, the height of the concentration step. Hence, this procedure, which is attractive because of its

TABLE I  
PARAMETERS OF THE VAN DEEMTER EQUATION

Column	$C_0$ (mg/ml)	$k'_0$	$D_s$	$k_t$
Vydac (with 2-phenylethanol)	0	0.88	$0.0016u_0 + 0.00025$	800
	20		$0.0016u_0 + 0.00024$	542
Laboratory-made (with 4- <i>tert.</i> -butylphenol)	0	10	$0.003u_0 + 0.00032$	83
	20		$0.003u_0 + 0.00035$	48

simplicity and good reproducibility, was used in this work.

As the band width in linear chromatography, the thickness of the shock layer can be expressed in either time or volume units. As we study the influence of the flow velocity on this thickness, it is more appropriate to use a distance or volume unit, which accounts automatically for the trivial effect of the change in the time scale when the mobile phase velocity is adjusted. As the procedure described gives  $\Delta\eta_t$ , we obtain  $\Delta\eta_x$  by multiplying the former by the shock velocity,  $U_s = u/(1 + K)$ .

## RESULTS AND DISCUSSION

We determined the SLT in single-component frontal analysis using two compounds and three columns of different lengths, packed with the same stationary phase. Shock layers are much narrower than either the small sample size peaks, or the breakthrough curves of small concentration steps which are recorded under the same experimental conditions, but correspond to linear chromatography. We see in eqn. 5 that, for values of  $\Gamma_0$  between 0.1 and 1, corresponding to moderate to heavy column loading, the SLT is between 50 and 7 times the efficiency contribution, itself of the same order as the column HETP. Accordingly, SLTs are more difficult than band widths to measure accurately. For this reason, some discrepancies are noted between the experimental results and theoretical predictions. Such discrepancies are more prone to take place at high velocities, because of the difficulty in eliminating extra-column band broadening.

It should be noted that the thickness of the shock layer cannot become larger than the width of the breakthrough curve under linear conditions. This width is of the order of  $q\sigma$  or, in distance terms,  $q\sqrt{HL}$ ,  $q$  (a numerical parameter) depending on the value selected for  $\theta$ , with  $\text{erf}(q) = \theta$ . In this work,  $q$  was equal to 2.15, corresponding to the width of a Gaussian curve at 10% of its height. However, eqns. 5 predict that SLT tends towards infinity when  $\Gamma_0$ , and hence  $C_0$ , tends towards 0 (since  $K$  tends towards  $k'_0$ ). This incorrect result comes from the fact that eqns. 5 are valid only when the shock

layer is fully formed. In linear chromatography, there is no shock or shock layer, and eqns. 5 are not valid. In the transition region, when the radius of curvature of the isotherm is very large but no longer infinite, a shock layer could exist, but it takes a very long column for this shock layer to form. If the actual column used is too short, the breakthrough curve recorded is not the shock layer profile, it is narrower, and the experimental result cannot be expected to fit with the theory.

### *Dependence of the thickness of the shock layer on the mobile phase velocity*

Experimental determination of the shock layer is difficult. The signal must be recorded precisely and sources of signal noise carefully controlled. The study also requires an accurate measurement of the adsorption isotherm (to derive the isotherm parameter  $b$ ), and of the dependence of the HETP on the mobile phase velocity (to derive the parameters of the Van Deemter equation, eqn. 11a). As a consequence, a significant amount of random fluctuations is expected.

In Figs. 2 and 3, we show for each of the two columns studied the plots of the column HETP *versus* the mobile phase flow velocity and of the shock layer thickness for a constant concentration step height *versus* the same velocity. The experimental results (symbols) are compared with the prediction of eqn. 5b (solid line), which is overlaid. In all instances, the agreement between the experimental results and the prediction of eqn. 5b is satisfactory over the whole range of velocities of interest in practical applications. The slightly faster rate of increase of the shock layer thickness at high flow velocities may be attributed to an instrumental contribution (response time of the detector). This result demonstrates the validity, in the experimental cases studied, of eqn. 5b.

The plots of SLT and HETP *versus* the flow velocity are similar. Both exhibit a minimum. We observe, however, that the minima of the two curves are not obtained for the same velocity. This can be explained by comparing eqns. 9 and 10. HETP in linear chromatography is given by eqns. 11a and b. It includes two terms. The first term of eqn. 10 is the sum of the axial diffusion,  $2\gamma D_m/u$  (where  $\gamma$  is the tortuosity coefficient and



$D_m$  the molecular diffusivity of the solute in the mobile phase) and the eddy diffusion ( $A$  in the Van Deemter equation,  $Au^{1/3}$  in the Knox equation; see eqns. 11 and 12). The second term in eqn. 10 accounts for the rate of mass transfer [32,35,36]. As  $k_f$  is a lumped coefficient, this term includes the effects of diffusion through the stationary phase particles and the rate of adsorption/desorption.

Assuming a Van Deemter plate height equation (eqns. 11a and 12a), the first term is constant, the second term is proportional to  $1/u$  and the third term is proportional to  $u$ . Hence there is an optimum value of the mobile phase velocity for which the  $H$  is minimum and the column efficiency maximum:

$$u_{opt}^L = \sqrt{\frac{\gamma D_m (1 + k'_0)^2 k_f}{k'_0}} \quad (14)$$

This is a classical result. If we consider now eqn. 5b, we see that, assuming that  $D_L$  is again given by eqn. 12a, only the first factor on the right-hand side depends on the mobile phase velocity. Differentiating it with respect to  $u$  yields an optimum value of the velocity:

$$u_{opt}^S = \sqrt{\frac{\gamma D_m (1 + K)^2 k_f}{K}} \quad (15)$$

The two equations are obviously very similar, but because of the non-linear thermodynamics of phase equilibrium, the second one depends on the height of the concentration step and also on the second isotherm parameter. Therefore, for a given system, there exists an optimum linear velocity which gives the smallest shock layer thickness for a given step concentration. This optimum velocity is a function of the concentration and differs from the optimum velocity under linear conditions.

We note also that when the mobile phase velocity increases indefinitely, the shock layer in time units,  $\Delta\eta_t$  (eqn. 5c), tends towards a finite limit. This limit is inversely proportional to  $k_f$ .

*Dependence of the optimum mobile phase velocity  $u_{opt}^S$  on the height of the concentration step*

Figs. 4 (2-phenylethanol) and 5 (4-*tert*-butylphenol) show the plots of the optimum flow

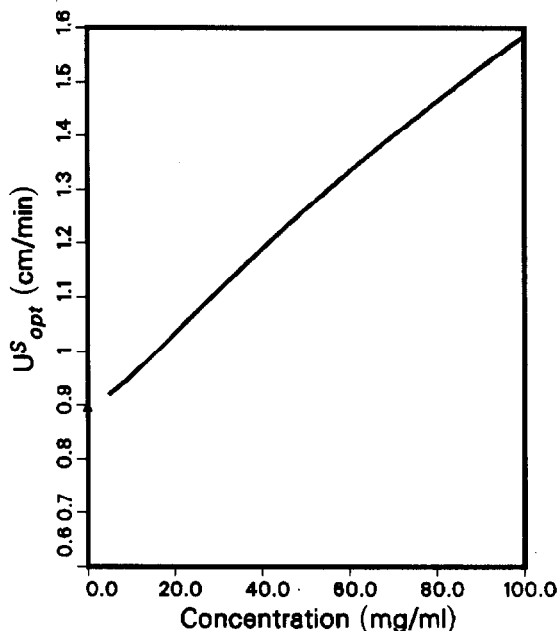


Fig. 4. Plot of the optimum velocity for minimum shock layer thickness versus the height of the concentration step (eqn. 15). Sample, 2-phenylethanol ( $k'_0 = 0.88$ ). Experimental conditions as in Fig. 2. The symbol  $\Delta$  gives  $u_{opt}^L$ , the optimum velocity for minimum HETP.

velocity versus the height of the concentration step for the two compounds studied. Both curves have a limit equal to  $u_{opt}^L$  for  $\Gamma_0 = C_0 = 0$ , which is obvious from eqns. 14 and 15. However, these two curves are strikingly different. One exhibits a well defined minimum, whereas the other is steadily increasing with increasing concentration.

Eqn. 15 shows that the optimum velocity for minimum shock layer thickness is a function of the height of the concentration step. Differentiation of eqn. 15 with respect to  $\Gamma_0$  shows that the optimum velocity,  $u_{opt}^S$ , passes through a minimum, achieved at the concentration

$$\Gamma_0^* = k'_0 - 1 \quad (16a)$$

$$C_0^* = \frac{k'_0 - 1}{b} = Fq_s \cdot \frac{k'_0 - 1}{k'_0} \quad (16b)$$

The difference between the curves in Figs. 4 and 5 is now easily explained. There is obviously no minimum of  $u_{opt}^S$  when  $k'_0$  is smaller than unity; then the optimum velocity for minimum SLT increases regularly with increasing concentration step height. For the value of  $\Gamma_0$  given by eqn.

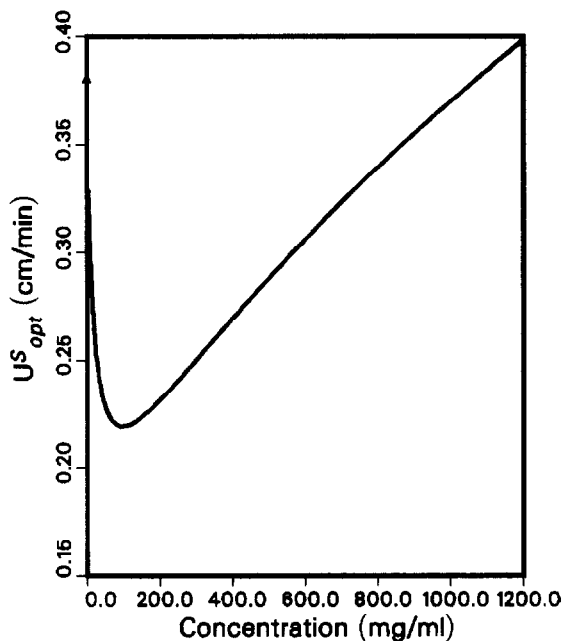


Fig. 5. Plot of the optimum velocity for minimum shock layer thickness versus the height of the concentration step. Sample, 4-*tert.*-butylphenol ( $k'_0 = 10$ ). Experimental conditions as in Fig. 3. The symbol  $\Delta$  gives  $u_{opt}^L$ , the optimum velocity for minimum HETP. The concentration for which  $u_{opt}^S = u_{opt}^L$  is 97 mg/ml.

16a,  $K$  is equal to 1 and  $u_{opt}^S$  is smaller, or much smaller, than  $u_{opt}^L$ .

By equating eqns. 14 and 15, we obtain the concentration step height at which the optimum linear velocity for minimum SLT is equal to that for minimum HETP. We have two solutions,  $\Gamma_0 = 0$  (a trivial solution) and

$$\Gamma_0^{**} = k_0'^2 - 1 \quad (17a)$$

$$C_0^{**} = Fq_s \left( k_0' - \frac{1}{k_0'} \right) \quad (17b)$$

We have shown above that the velocity for which the shock layer thickness is minimum depends on the height of the concentration step and is given by eqn. 15. We have also shown that the two optimum velocities,  $u_{opt}^S$  for minimum shock layer thickness and  $u_{opt}^L$  for minimum HETP, are equal for  $\Gamma_0 = k_0'^2 - 1$ . At lower concentrations, we have  $u_{opt}^S < u_{opt}^L$ , and the column should be operated at lower velocities in frontal analysis

than under linear conditions. When the concentration step exceeds  $k_0'^2 - 1$ , however, the converse is true, and the column should be operated at a higher flow velocity in frontal analysis than under linear conditions.

These results are illustrated in Figs. 4 and 5. It can be seen that part of or the whole of the concentration range discussed above is often inaccessible. The only exception is when the retention factor of the component selected is smaller than about 2 and the column saturation capacity is large. For example, for 2-phenylethanol (Fig. 4) the retention factor is lower than unity, the optimum mobile phase velocity for minimum SLT always increases with increasing concentration step height and  $u_{opt}^S$  always markedly exceeds  $u_{opt}^L$ . In contrast, for 4-*tert.*-butylphenol (Fig. 5), which has a large retention factor ( $k'_0 = 10$ ), the optimum velocity for minimum shock layer thickness decreases with increasing concentration until  $C_0 = 97$  mg/ml, where it is minimum, and then increases. With this compound,  $u_{opt}^S$  is lower than  $u_{opt}^L$  until  $C_0$  reaches the impractical concentration of 1080

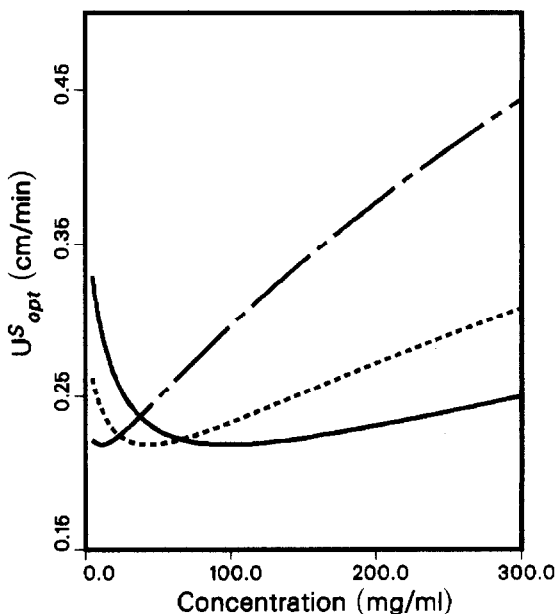


Fig. 6. Plot of the optimum velocity for minimum shock layer thickness versus the height of the concentration step (eqn. 15). Dash-dotted line,  $k'_0 = 2$ ; dotted line,  $k'_0 = 5$ ; solid line,  $k'_0 = 10$ .

mg/ml. In the range of concentrations accessible to experiments,  $u_{\text{opt}}^{\text{S}}$  will be much lower than  $u_{\text{opt}}^{\text{L}}$ .

Fig. 6 illustrates the important differences between the behavior of the SLT of different compounds with the height of the concentration step. When the retention factor,  $k'_0$ , is low, the optimum velocity for minimum SLT increases constantly with increasing concentration. When the retention factor exceeds about 2, the optimum velocity exhibits a minimum for a certain concentration, and this concentration increases with increasing value of the retention factor.

#### *Dependence of the thickness of the shock layer on the height of the concentration step*

The SLT depends on the height of the concentration step. However, differentiation of eqn. 5b with respect to  $\Gamma_0$  and setting the differential equal to zero gives a fourth-degree equation without simple roots. We can have an idea of the variation of  $\Delta\eta_t$ , however, by studying separately the two terms.

Differentiation of the first term  $[(1+K)/K][(I_0+2)/I_0]$ , with respect to  $\Gamma_0$  shows that it is minimum for

$$\Gamma_{0,1} = \sqrt{2(1+k'_0)} \quad (18a)$$

This concentration is high. For  $k'_0 = 1$ , which is a very small value of the retention factor by displacement standards, the value of  $\Gamma_{0,1}$  is 2, for which value we achieve a coverage of two-thirds of a monolayer at equilibrium (see eqn. 6b). For  $k'_0 = 7$ , a surface coverage of 80% would be obtained at the optimum concentration of 4. As a consequence, we can expect that this term will decrease with increasing height of the concentration step in the entire range of practical interest.

Similarly, differentiation of the second term of eqn. 5b,  $[1/(1+K)][(I_0+2)/I_0]$ , shows that it is minimum for

$$\Gamma_{0,2} = \frac{2 + \sqrt{4 + 2(k'_0{}^2 - 2)(k'_0 + 1)}}{k'_0{}^2 - 2} \quad (18b)$$

For  $k'_0 > \sqrt{2}$ , the value of  $\Gamma_{0,2}$  is large. For  $k'_0 = 2$ ,  $\Gamma_{0,2} = 3$ , for which the surface coverage at equilibrium is 75%. For  $k'_0 < \sqrt{2}$ , the second

term of eqn. 5b decreases monotonically with increasing concentration.

As both terms of eqn. 5b decrease with increasing value of  $C_0$  until they are minimum for impractically large concentrations, we can conclude that the same is true for the SLT, which in practice will decrease steadily with increasing height of the concentration step.

We measured the shock layer thickness of a series of breakthrough curves recorded for the injection of solutions of increasing concentrations in a column previously swept with pure mobile phase, so the height of the concentration step is always  $C_0$ . Between two successive experiments, the column is properly swept with pure mobile phase during the time needed to purge it from the solute introduced previously. The experimental data obtained with the Vydac column are shown in Fig. 7a (symbols). They are overlaid in this figure with the curve derived from eqn. 5b (solid line). There is very good agreement between the experimental results and the prediction of eqn. 5b at high concentrations. At low concentrations, this equation predicts a shock layer thickness that is thicker than the width of a breakthrough front under linear conditions, and significant deviations take place.

The dotted and dashed lines in Fig. 7a correspond to the two contributions to the shock layer thickness in eqn. 5b. These contributions result from the axial dispersion and the mass transfer resistance, respectively. They were calculated from the sum of the *A* and *B* terms and the *C* term of the Van Deemter equation [33] (eqns. 12a and c and Table I). Whereas the contribution of the mass transfer resistance decreases monotonically with increasing concentration, the contribution of the axial dispersion passes through a minimum, which explains the minimum in the shock layer thickness. We note that, under the experimental conditions of Fig. 7a, eqns. 5 and 16 predict a minimum for the thickness of the shock layer for a concentration step of *ca.* 20 mg/ml, in agreement with the experimental data.

The same data are shown in Fig. 7b, where the choice of a logarithmic scale for the concentration axis permits a clearer illustration of the experimental results obtained in a concentration

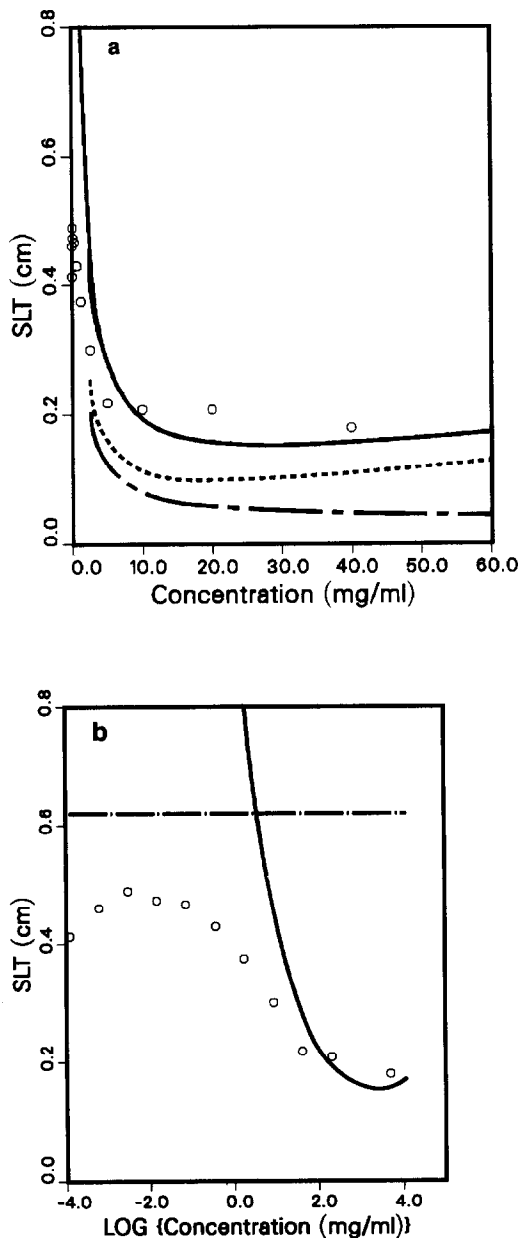


Fig. 7. Plot of the shock layer thickness *versus* the height of the concentration step of 2-phenylethanol. Experimental conditions as in Fig. 2 except the flow velocity, 0.07 cm/s. At this flow-rate,  $H = 4.8 \cdot 10^{-3}$  cm, under linear conditions. (a) Symbols, experimental data; solid line, eqn. 5b; dotted line, contribution of axial dispersion to the height of the shock layer; dashed line, contribution of mass transfer resistance to the height of the shock layer. (b) Symbols, experimental data in semi-logarithmic coordinates; dot-dashed line, value predicted by the linear model ( $\omega = 4\sqrt{HL} = 0.62$  cm); solid line, variation predicted by eqn. 5b.

range covering 3.5 orders of magnitude. The existence of three concentration domains is obvious. At high concentrations, eqn. 5b fits the experimental results well. At very low concentrations, on the other hand, the width of the breakthrough front is constant and equal to the value resulting from measurements of the width of the Gaussian peak obtained under linear conditions. There is an intermediate concentration range in which the width of the breakthrough curve decreases sharply with increasing height of the concentration step.

As mentioned above, eqns. 5 correspond to a constant pattern behavior, *i.e.*, to an asymptotic solution. In other words, these equations are strictly valid only for an infinitely long column. The rate at which a breakthrough profile converges towards a constant pattern decreases with decreasing step height, and hence with decreasing change in isotherm slope across the step. At the end of a finite column, we observe a breakthrough curve that is close to a constant pattern, and hence has the shock layer profile, only if the column is long enough and the concentration step high enough. If the column is too short or the step height too small, a constant pattern is not achieved, and the width of the breakthrough curve is narrower than predicted by eqn. 5b. This is in agreement with the experimental results in the figures.

## CONCLUSIONS

An optimum linear velocity for minimum thickness of the shock layer exists in frontal analysis. This optimum velocity is a function of the height of the concentration step. Depending on the retention of the compound under infinite dilution, the optimum velocity increases constantly with increasing height of the concentration step, or may pass through a minimum.

Accordingly, when measuring adsorption isotherms by frontal analysis, the mobile phase velocity should be selected carefully. When the retention factor under linear conditions is much higher than unity, relatively low values of the mobile phase velocity, lower than the optimum velocity for minimum plate height, should be considered, especially for the small step heights.

However, the most important consequences of a study of the dependence of shock layer thicknesses on the mobile phase velocity and the height of the concentration step will be found in displacement chromatography [24]. As this problem is a binary problem, it must be discussed in connection with the theory of shock layers between two components.

## SYMBOLS

$a, b$	Coefficients of the Langmuir isotherm
$A, B$	Coefficients in the plate height equation
$C$	Concentration in the mobile phase (mg/ml)
$C^l$	Concentrations in the column at $x = -\infty$
$C^r$	Concentrations in the column at $x = +\infty$
$C_1^*$	Concentration bound of the shock layer, on the upstream side
$C_r^*$	Concentration bound of the shock layer, on the downstream side
$C_0$	Concentration of a step injection
$D_a$	Apparent dispersion coefficient
$D_L$	Axial dispersion coefficient ( $\text{cm}^2/\text{s}$ )
$F$	Phase ratio of the column (ml/ml)
$f(C)$	Isotherm equation
HETP, $H$	Height equivalent to a theoretical plate (cm)
$K$	Auxiliary parameter
$k_f$	Rate constant of mass transfer ( $\text{s}^{-1}$ )
$k'_0$	Capacity factor of the component at infinite dilution
$L$	Column length
$Q$	Concentration in the stationary phase (mg/ml)
$q_s$	Column saturation capacity
SLT	Shock layer thickness
$t$	Time
$U_s$	Shock layer velocity (cm/min)
$u$	Mobile phase linear velocity (cm/s)
$u_{\text{opt}}^L$	Optimum linear velocity in linear chromatography (cm/s)
$u_{\text{opt}}^S$	Optimum linear velocity for minimum shock layer thickness (cm/s)
$x$	Reduced distance along the column
$z$	Distance along the column

## Greek letters

$\Gamma$	Dimensionless mobile phase concentration
$\gamma$	Tortuosity of the packing
$\Delta\eta_x$	Shock layer thickness in length units (cm)
$\Delta\eta_t$	Shock layer thickness in time units (s)
$\Delta Q$	Concentration amplitude of the shock layer in the stationary phase
$\Delta C$	Concentration amplitude of the shock layer in the mobile phase
$\Delta\xi$	Dimensionless shock layer
$\lambda$	Reduced shock velocity
$\Lambda$	Dimensionless stationary phase concentration
$\theta$	Parameter defining the shock layer thickness
$\sigma$	Standard deviation of a Gaussian peak
$\tau$	Reduced time
$\xi$	Moving coordinate of the shock layer

## ACKNOWLEDGEMENTS

We gratefully acknowledge the gift by the Separation Group (Hesperia, CA) of the column and the packing material used in this work. This work was supported in part by grant CHE-9201663 from the National Science Foundation and by the cooperative agreement between the University of Tennessee and the Oak Ridge National Laboratory. We acknowledge support of our computational effort by the University of Tennessee Computing Center.

## REFERENCES

- 1 B.A. Bidlingmeyer, *Preparative Liquid Chromatography*, Elsevier, Amsterdam, 1987.
- 2 H. Colin, *Sep. Sci. Technol.*, 22 (1987) 1953.
- 3 J.E. Eble, R.L. Grob, P.E. Antle and L.R. Snyder, *J. Chromatogr.*, 384 (1987) 25.
- 4 J.E. Eble, R.L. Grob, P.E. Antle and L.R. Snyder, *J. Chromatogr.*, 384 (1987) 31.
- 5 J.H. Knox and M. Pyper, *J. Chromatogr.*, 363 (1986) 1.
- 6 S. Golshan-Shirazi and G. Guiochon, *Anal. Chem.*, 60 (1988) 2364.
- 7 S. Golshan-Shirazi and G. Guiochon, *Anal. Chem.*, 61 (1989) 462.

- 8 C.A. Lucy and P.W. Carr, *J. Chromatogr.*, 556 (1991) 159.
- 9 E.V. Dose and G. Guiochon, *Anal. Chem.*, 62 (1990) 1723.
- 10 A.M. Katti and G. Guiochon, *Adv. Chromatogr.*, 31 (1991) 1.
- 11 S. Golshan-Shirazi and G. Guiochon, in F. Dondi and G. Guiochon (Editors), *Theoretical Advancement in Chromatography and Related Separation Techniques (NATO ASI Series, Series C, Vol. 383)*, Kluwer, Dordrecht, 1992, pp. 1–33.
- 12 B.C. Lin, S. Golshan-Shirazi, Z. Ma and G. Guiochon, *Anal. Chem.*, 60 (1988) 2647.
- 13 T. Vermeulen, *Adv. Chem. Eng.*, 2 (1958) 147.
- 14 F. Helfferich, *Ion Exchange*, McGraw-Hill, New York, 1962, Ch. 9.
- 15 D.O. Cooney and E.N. Lightfoot, *Ind. Eng. Chem. Fundam.*, 5 (1966) 212.
- 16 T. Vermeulen, M.D. LeVan, N.K. Hiester and G. Klein, in R.H. Perry, C.H. Chilton and S.D. Kirkpatrick (Editors), *Chemical Engineers' Handbook*, Academic Press, New York, 4th ed., 1963, Sect. 16.
- 17 N.K. Hiester and T. Vermeulen, *Chem. Eng. Prog.*, 48 (1958) 505.
- 18 H.-K. Rhee, B.F. Bodin and N.R. Amundson, *Chem. Eng. Sci.*, 26 (1971) 1571.
- 19 H.-K. Rhee and N.R. Amundson, *Chem. Eng. Sci.*, 27 (1972) 199.
- 20 H.-K. Rhee and N.R. Amundson, *Chem. Eng. Sci.*, 28 (1973) 55.
- 21 H.-K. Rhee and N.R. Amundson, *Chem. Eng. Sci.*, 29 (1974) 2049.
- 22 Z. Ma and G. Guiochon, *J. Chromatogr.*, 603 (1992) 13.
- 23 Z. Ma and G. Guiochon, *J. Chromatogr.*, 609 (1992) 19.
- 24 J. Zhu and G. Guiochon, in preparation.
- 25 Cs. Horváth, A. Nahum and J.H. Frenz, *J. Chromatogr.*, 218 (1981) 365.
- 26 Cs. Horváth, J. Frenz and Z. El Rassi, *J. Chromatogr.*, 255 (1983) 273.
- 27 J. Frenz, Ph. Van Der Schrieck and Cs. Horváth, *J. Chromatogr.*, 330 (1985) 1.
- 28 J. Frenz and Cs. Horváth, in Cs. Horváth (Editor), *High-Performance Liquid Chromatography—Advances and Perspectives*, Vol. 5, Academic Press, New York, 1988, pp. 211–314.
- 29 F. Cardinali, A. Ziggotti and G.C. Viscomi, *J. Chromatogr.*, 499 (1990) 37.
- 30 G. Subramanian, M.W. Phillips and S.M. Cramer, *J. Chromatogr.*, 454 (1988) 1.
- 31 G. Subramanian and S.M. Cramer, *Biotechnol. Prog.*, 454 (1989) 1.
- 32 S. Golshan-Shirazi and G. Guiochon, *J. Chromatogr.*, 603 (1992) 1.
- 33 J.J. Van Deemter, F.J. Zuiderweg and A. Klinkenberg, *Chem. Eng. Sci.*, 5 (1956) 271.
- 34 J.H. Knox and M. Saleem, *J. Chromatogr. Sci.*, 7 (1969) 745.
- 35 G. Guiochon, S. Golshan-Shirazi and A. Jaulmes, *Anal. Chem.*, 60 (1988) 1856.
- 36 J.C. Giddings, *Dynamics of Chromatography*, Marcel Dekker, New York, 1964.
- 37 S. Golshan-Shirazi, S. Ghodbane and G. Guiochon, *Anal. Chem.*, 60 (1988) 2630.